Some Aspects of Two-Phase Flows with Mixing and Combustion in Bounded and Unbounded Flows

JOHN GENOVESE,* RAYMOND B. EDELMAN,† AND OWEN F. FORTUNE‡
General Applied Science Laboratories Inc., Westbury, N. Y.

An analysis is presented for the multiphase axisymmetric or plane two-dimensional mixing and combustion of a flowfield comprised of particulate matter suspended in a gaseous medium. Applications are found in propulsion systems, wind tunnels, stationary power plants, and the general area of pollution. These problems involve a number of coupled rate processes, including homogeneous and heterogeneous chemical kinetics, phase transition and mixing both within and between the phases present in the system. The conservation equations for mass, momentum, energy, and interphase mass transport are described. The equations are solved by a computerized, explicit, finite-difference technique. Results are presented for two sets of assumptions: finite-rate combustion with equilibrium phase transition applied to an air-liquid hydrogen system, and equilibrium combustion with finite-rate phase transition for an air-hydrocarbon fuel system. Based on the particle sizes encountered, the turbulent transport of particulate matter will range from zero mixing for large particles to a condition of diffusive equilibrium for small particles. The possibility of phase separation is shown to be an important consideration in multiphase flows with chemical reactions.

Nomenclature

g = mass fraction of condensate
h = static enthalpy
H = stagnation enthalpy
J = nucleation rate
k = Boltzman constant
$\mathfrak{M}$ = molecular weight
M_L = mass of a molecule
n^* = number of molecules in a critical droplet
N = number density of particles
n_s = all chemically reacting species
p = pressure
p_v = partial pressure of the vapor
$p_{v\infty}$ = equilibrium partial pressure
Pr = Prandtl number
r = radius
r^* = radius of a critical drop
r_s = Sauter radius
R_0 = universal gas constant
s = accommodation coefficient
Sc = Schmidt number
T = temperature
u,v = axial and vertical velocity components
w^* = work of creation of a critical droplet
$\dot{W}$ = rate of production
x,y = axial and vertical coordinates
α = mass fraction
ρ = density
σ = surface tension
μ = viscosity coefficient
φ = saturation ratio, $p_v/p_{v\infty}$
ψ = stream function

Subscripts

i,j = chemical species and chemical element, respectively
g,m = gas and mixture, respectively
L,v = condensate and condensible vapor, respectively

Presented as Paper 70-145 at the AIAA 8th Aerospace Sciences Meeting, New York, January 19–21, 1970; submitted February 19, 1970; revision received September 15, 1970. This work was supported by NASA under Contracts NAS8-2686 and NAS8-21264.

* Senior Scientist. Member AIAA.
† Manager, Thermochemistry and Viscous Flow Section. Member AIAA.
‡ Project Scientist. Member AIAA.

Introduction

MANY practical systems involve the flow of fluids containing particles in suspension. Such multiphase flows are relevant to problems ranging from propulsion system component design to the description of the formation and dispersion of pollutants from various industrial process equipment. Generally, the related flows involve a number of coupled processes including homogeneous gas phase chemical reactions, heterogeneous chemical reactions, phase transition, and mixing within and between the phases.

Much of the two-phase flow literature of the past ten years was focussed upon basic flow configurations such as nozzle flows and shocks.[1–4] In general, they treated cases involving inert particles suspended in an otherwise inviscid or laminar-like fluid. More recently, however, attempts have been made to treat problems including effects of mixing and combustion in turbulent flows.[5–8] This paper presents the results of studies designed to demonstrate some effects of chemical and particulate phase mixing models that have not been treated in the past. In particular, the work includes two limiting conditions based upon practical applications: a) conditions where finite-rate combustion and equilibrium phase transition are appropriate, and b) applications where equilibrium combustion and finite-rate phase transition are suitable. In addition, turbulent transport of the particulate matter is considered in two limits: 1) equilibrium diffusion where the gas phase and particulate phase diffusivities are equal, and 2) frozen diffusion where the particulate phase diffusivities are zero and the particles do not diffuse.

Analysis

For a multiphase system one must describe not only the conservation of mass, momentum, and energy for the con-

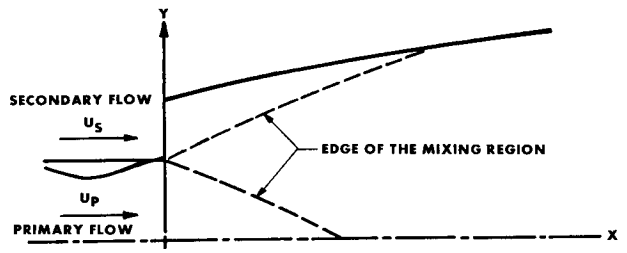

Fig. 1 Schematic of the configuration examined in the equilibrium diffusion analysis.

densed phase, but also the dynamic and thermodynamic interactions between the phases. In general, this involves the description of velocity differences (dynamic nonequilibrium), temperature differences (thermal nonequilibrium), and mass transfer between the phases (nonequilibrium phase change).[9]

In this investigation we are concerned with phase transition in systems involving mixing and combustion, with emphasis on interphase mass transfer under the assumption of dynamic and thermal equilibrium for the mean components of velocity and temperature. These assumptions have been investigated in the past,[7-10] and it has been demonstrated that in certain turbulent diffusive flows the system can be characterized by a single mean velocity and temperature, whereas the particles may diffuse at rates different from those of the gas-phase components.[9] The treatment of such flows is of interest in connection with configurations of the type shown schematically in Fig. 1. These flows may be bounded or unbounded where diffusion is important only in the lateral direction and pressure gradients are important only in the streamwise direction.

Finite Rate Condensation in Diffusive Equilibrium with Simple Chemistry

When a multiphase flow is generated by the process of condensation from the vapor phase, the system will contain a distribution of very small particles. The condensation process involves the formation of critically sized nuclei and their subsequent growth. Even after a substantial growth period, the bulk of the condensate will be of submicron size. Under this condition, the particles can easily respond to the mean and fluctuating components of the gas phase motion and the concept of diffusive equilibrium becomes applicable.

The present discussion will emphasize this finite-rate condensation process in diffusive flows. Either CO_2 or H_2O is considered as the potential condensible in the flowfield where the rate of condensation is based upon classical nucleation and growth theory.[11,12] In addition to finite-rate condensation, chemical reactions are included in terms of a quasi-complete combustion model appropriate for hydrocarbon systems. This combustion model includes the fuel,

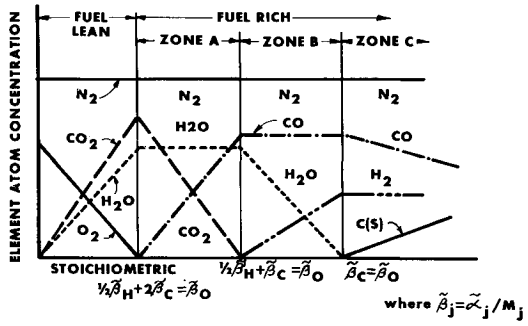

Fig. 2 Quasi-complete combustion hydrocarbon-air chemistry.

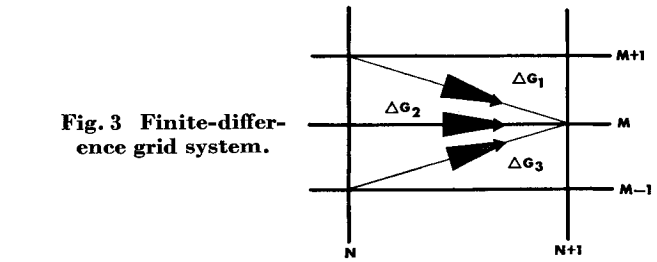

Fig. 3 Finite-difference grid system.

CO, CO_2, H_2, H_2O, and $C_{(solid)}$ depending upon the local equivalence ratio as shown in Fig. 2. This model is based upon the behavior of the most important equilibrium species tabulated in Ref. 13. This model gives a reasonable approximation to diffusion controlled combustion flowfields, but it should be noted that more exact equilibrium calculations may be coupled to the flowfield with no change in the basic analysis or solution techniques.

The describing equations for this flow are given in Ref. 5

Continuity

$$\partial(\rho_m u y^N)/\partial x + \partial(\rho_m v y^N)/\partial y = 0 \tag{1}$$

where

$$N = \begin{cases} 0 \text{ two-dimensional} \\ 1 \text{ axisymmetric} \end{cases}$$

Momentum

$$\rho_m u(\partial u/\partial x) + \rho_m v(\partial u/\partial y) = -(dp/dx) + (1/y^N)(\partial/\partial y)[\mu_m y^N(\partial u/\partial y)] \tag{2}$$

Energy

$$\rho_m u(\partial H_m/\partial x) + \rho_m v(\partial H_m/\partial y) = (1/y^N)(\partial/\partial y) \times \{y^N \mu_m[(1/Pr)(\partial H_m/\partial y) + (1 - 1/Pr) \times [(\partial u^2/2)/\partial y] + \Sigma\,(1/Sc - 1/Pr)h_m{}^i\,\partial\alpha_i/\partial y]\} \tag{3}$$

The analysis requires specification of either the wall contour or the static pressure as a function of the downstream coordinate.

Since an equilibrium combustion chemistry model is used to describe the burning process in the present case, the species participating in the reactions are cast in the form of element mass fractions. The condensate acts as a diluent in the local burning process and remains in specie mass fraction form. Thus the diffusion equation can be split into parts. Element mass fractions of the chemically reacting species $j = C, O_2, H_2, N_2$;

$$\rho_m u \frac{\partial \alpha_j}{\partial x} + \rho_m v \frac{\partial \alpha_j}{\partial y} = \frac{1}{y^N}\frac{\partial}{\partial y}\frac{y^N \mu_m}{Sc}\frac{\partial \alpha_j}{\partial y} + \dot{W}_j \tag{4}$$

Mass fraction of the species condensing out of the vapor

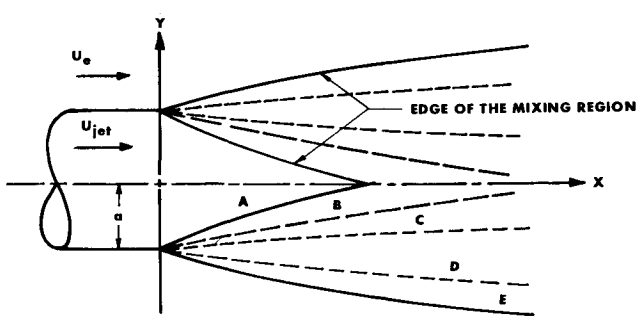

Fig. 4 Schematic of the configuration examined in the frozen diffusion analysis.

phase $\alpha_L = CO_2$ or H_2O,

$$\rho_m u(\partial\alpha_L/\partial x) + \rho_m v(\partial\alpha_L/\partial y) = (1/y^N)(\partial/\partial y)[(y^N\mu_m/Sc)(\partial\alpha_L/\partial y)] + \dot{W}_L \quad (5)$$

where

$$\sum_{j=1}^{4} \alpha_j + \alpha_L = 1 \text{ and } \alpha_j = \sum_{i=1}^{n_s} \nu_{ij} \frac{\mathfrak{M}_j}{\mathfrak{M}_i} \alpha_i \quad (6)$$

The production rate of element mass fractions can be expressed as

$$\dot{W}_j = \sum_{i=1}^{n} \nu_{ij} \frac{\mathfrak{M}_j}{\mathfrak{M}_i} \dot{W}_i \quad (7)$$

Initial and boundary conditions

$$\left.\begin{aligned} &0 \le y \le y_p \begin{cases} u = u_p(y) \\ T = T_p(y) \\ \alpha_j = \alpha_{jp}(y) \\ \alpha_L(r) = \alpha_{Lp}(r,y) \end{cases} \\ &y_p < y \le y_w \begin{cases} u = u_s(y) \\ T = T_s(y) \\ \alpha_j = \alpha_{js}(y) \\ \alpha_L(r) = \alpha_{Ls}(r,y) \end{cases} \end{aligned}\right\} \text{ for } x = 0 \text{ or } \left\{\begin{aligned} &\frac{\partial\alpha_i}{\partial y} = 0 \\ &\frac{\partial H_m}{\partial y} = 0 \\ &T = T_w(x) \text{ and} \\ &\frac{\partial u}{\partial y} = \left(\frac{\rho u^2}{\mu}\right) C_f/2 \end{aligned}\right\} \text{ for } \begin{matrix} x \ge 0 \\ \text{and} \\ y = y_w \end{matrix} \quad (8)$$

for all x at $y = 0$ $v = \partial\alpha_i/\partial x = \partial T/\partial y = \partial u/\partial x = 0$, where the subscripts p, s, and w refer to primary stream, secondary stream, and wall values, respectively.

The contribution of the condensate to the system static pressure is neglected and the ideal gas law for the mixture becomes

$$p = \rho_m R_0 T \sum_{i=1}^{n} \frac{\alpha_i}{\mathfrak{M}_i} \quad (9)$$

where n = all gases in the mixture. This formulation was implemented for digital computation in terms of the von Mises coordinates[14]:

$$\psi^N(\partial\psi/\partial y) = \rho_m u y^N \quad (10)$$

$$\psi^N(\partial\psi/\partial x) = -\rho_m v y^N \quad (11)$$

Condensation Kinetics

The condensation process is initiated by the formation of critical sized clusters of molecules in the new phase. This nucleation process can be of two general types: homogeneous, where the new phase deposits on nuclei spontaneously formed when vapor molecules collide and stick; and heterogeneous, in which the condensate forms around foreign particles serving as centers for condensation. For simplicity the present analysis treats only the first of these phenomena, but the generalization needed to include heterogeneous nucleation is straightforward.[11,12]

The model for homogeneous nucleation, based on kinetic theory consists of specifying expressions for the radius of the critical droplets, the work required for their formation and a droplet growth law that governs their size history as they flow downstream. Based on the results of Ref. 12, we may write the following equations for these parameters:

$$r^* = 2\sigma M_L/\rho_L R_0 T \ln\varphi \quad (12)$$

$$w^* = (4\pi/3)\sigma r^{*2} \quad (13)$$

where $\varphi = p_v/p_{v\infty}$. The nucleation rate,

$$J = (p_v^2/\rho_L T^2)(3M_L/\pi\rho_L)^{1/3}(1/r^*)^2 * \exp[\tfrac{1}{2}\ln(2\sigma M_L/\pi) - 2\ln k - w^*] \quad (14)$$

determines the number of new droplets created per unit volume, per unit time. The pre-exponential factors are closely related to the collision frequency of vapor molecules, and the exponential is an expression for the work of cluster formation.

The growth law employed is capable of predicting the rate of droplet size increase for condensation ($\varphi > 1$). A simple growth law is given by kinetic theory in the form

$$dr/dx = (M_L/2\pi kT)^{1/2} s(p_v - p_v)/\rho_L u \quad (15)$$

where s is defined as the accommodation coefficient.

Particle Size Distribution

The combined effects of continuous nucleation, growth, and the nonuniform velocity and temperature fields provide conditions resulting in a spectrum of particle sizes at every point in the flow. To completely specify the production rate, $\dot{W}_L$, of condensate requires knowledge of this local particle size and number density distribution. To track the particle history through the flow, the total amount of condensate present at every point in the flowfield is divided into a set of categories based on particle size. Within each size range all the particles are combined to form an average with a volume to surface area ratio equal to that of the summation over-all contributions. This equivalent particle size is the Sauter mean value and is expressed as

$$r_s = \Sigma n_i r_i^3/\Sigma n_i r_i^2 \quad (16)$$

where n_i particles have radius r_i.

The mass fraction of each category is equal to the sum of the mass fractions of each contribution. With the average size of category particles and the total category mass fraction known, the appropriate number of equivalent particles is established for every class. This representation provides an exact equivalence for the subsequent rate process provided the rate of change of mass depends directly upon the particle surface area. This is the case when an expression of the type given by Eq. (15) is used.

The particle distribution array in terms of size, mass fraction, and number in each category at every grid point can only be altered by three phenomena: the creation of new droplets, the growth of old droplets, and the diffusion of droplets from the neighboring flow.

Whenever new particles are created by the condensation of droplets from the vapor phase, their size is defined in terms of the local pressure and temperature by Eq. (12). Based on the definition of the nucleation rate equation, the number density of new particles created over a given length is given by

$$N_s = \int_{x_0}^{x} \frac{J(x)}{u}\, dx \quad (17)$$

If we define n^* as the number of molecules in a critical drop, the mass fraction of condensate created over this step is:

$$g_s = \int (n^* M_L/\rho_m u) J(x) dx \text{ where } n^* = 4\pi r^{*3}\rho_L/3M_L \quad (18)$$

These particles are then categorized into the proper size group and averaged with those already in the category, using the Sauter criteria, to form a new class radius, mass fraction, and number density.

The radius of a droplet changes in accordance with the growth law as the flowfield develops. Thus after every step, the new droplet size is given by

$$r = r_0 + \int_{x_0}^{x} \frac{dr}{dx} dx \quad (19)$$

where the step size, Δx, is evaluated based on the stability criteria outlined in Ref. 14. Thus after every step the updated radius array must be reclassified in order to account for the transition of particles from one category to another. Since it is possible for more than one contribution to be made to a particular category, the total category mass must then be reaveraged, using the Sauter criteria, to establish the proper radius and number for the group. The particle array in terms of mass fraction, size, and number density resulting from the kinetics of the condensation process will be defined as

$$\begin{matrix} G(J,I)_k \\ R(J,I)_k \\ N(J,I)_k \end{matrix} \text{ at grid point } \begin{pmatrix} n+1 \\ m \end{pmatrix}$$

Each category in the particle array is altered by the diffusion of condensate of the same category from neighboring upstream locations. Subdividing the condensate mass fraction α_i into each category and treating the category mass fractions as separate species, the diffusion equation can be written in finite difference form of von Mises coordinates as

$$\alpha_{i,n+1,m} = \alpha_{i,n,m} + \Delta x \left(\frac{\dot{W}_i}{u}\right)_{n,m} + \frac{\Delta x}{\psi^N(\Delta\psi)^2}\left\{\left(\frac{b}{Sc_{n,m+1/2}}\right)\alpha_{i,n,m+1} - \left[\left(\frac{b}{Sc}\right)_{n,m+1/2} + \left(\frac{b}{Sc}\right)_{n,m+1/2}\right]\alpha_{i,n,m} + \left(\frac{b}{Sc}\right)_{n,m-1/2}\alpha_{i,n,m-1}\right\} \quad (20)$$

where the n, m subscripts refer to the grid point locations shown in Fig. 3.

The first term in Eq. 20 represents the change in α_i due to the condensation process as the flow moves downstream from n to $n+1$. The sum of the first two terms is the total mass fraction of category condensate present downstream due to kinetic processes, and the remaining term represents the contribution to the mass fraction from diffusion. Noting Fig. 3, the diffusional term can be split into the contributions from each of the three upstream points:

$$\Delta G_1 = \frac{\Delta x}{\psi^N(\Delta\psi)^2}\left(\frac{b}{Sc}\right)_{n,m+1/2}\alpha_{i,n,m+1} \quad (21)$$

$$\Delta G_2 = -\frac{\Delta x}{\psi^N(\Delta\psi)^2}\left[\left(\frac{b}{Sc}\right)_{n,m+1/2} + \left(\frac{b}{Sc}\right)_{n,m-1/2}\right]\alpha_{i,n,m} \quad (22)$$

$$\Delta G_3 = \frac{\Delta x}{\psi^N(\Delta\psi)^2}\left(\frac{b}{Sc}\right)_{n,m-1/2}\alpha_{i,n,m-1} \quad (23)$$

For each of the categories present at a given grid point, we may express the category mass fraction as

$$G(J,I)_{n+1,m} = \left[\Delta x\left(\frac{\dot{W}_i}{u}\right)_{n,m} + \alpha_{i,n,m}\right] + \Delta G_1 + \Delta G_2 + \Delta G_3 \quad (24)$$

where the kinetics contribution is evaluated as $G(J,I)_k$ with its associated $R(J,I)_k$ and $N(J,I)_k$. Knowing the category sizes associated with each upstream contribution the Sauter criteria can be used to define the new category radius:

$$R(J,I)_{n+1,m} = \frac{G(J,I)_k + \Delta G_1 + \Delta G_2 + \Delta G_3}{\dfrac{G(J,I)_k}{R(J,I)_k} + \dfrac{\Delta G_1}{R(J,I)_{n,m+1}} + \dfrac{\Delta G_2}{R(J,I)_{n,m}} + \dfrac{\Delta G_3}{R(J,I)_{n,m-1}}} \quad (25)$$

Knowing the new mass fraction and size, the number density of particles is determined from

$$N(J,I)_{n+1,m} = \frac{\rho_{n+1,m} G(J,I)_{n+1,m}}{4/3\pi\rho_L R(J,I)^3_{n+1,m}} \quad (26)$$

Some results of the application of this formulation are presented below.

Equilibrium Condensation with "Frozen" Diffusion

Insight into the extent the diffusion of particles effects the flowfield can be gained by considering the extreme limit of zero particle diffusion. This assumption is valid for laminar flow and turbulent flows involving large particles. Furthermore, the "equilibrium" and "frozen" diffusion models provide the bounds for the more general nonequilibrium problem.[9] The particular model described here includes homogeneous gas phase kinetics[15] with equilibrium phase transition in the limit of "frozen" diffusion.

The describing equations are similar in form to Eqs. (1–4). The essential difference appears in the diffusion terms where the mixture variables are replaced by the local gas phase variables. In addition, the species conservation equation replaces Eq. (4) and is given by

Species

$$\rho_m u\frac{\partial\alpha_i}{\partial x} + \rho_m v\frac{\partial\alpha_i}{\partial y} = \frac{1}{y_N}\left[\frac{\mu_g y^N}{Sc}\frac{\partial Y_i}{\partial x}\right] + \dot{W}_i \quad (27)$$

For this discussion the definition of the total specie mass fraction in terms of the vapor and condensate is given by

$$\alpha_i = (Y_i\rho_g + x_i\rho_L)/\rho_m \quad (28)$$

where

$$Y_i = \rho_{gi}/\rho_g \text{ for the vapors}$$
$$x_i = \rho_{Li}/\rho_L \text{ for the condensate} \quad (29)$$

The ideal gas law applied to the two-phase mixture assumes that contributions to the static pressure from the condensed species can be neglected.

$$p = \rho_m R_0 T \Sigma\alpha_i/\mathfrak{M}_i \quad (30)$$

where the summation extends over all gas phase mass fractions. Initial and boundary conditions for the free jet depicted in Fig. 4

$$\text{at } x=0 \begin{cases} 0 \le y \le a & \begin{cases} u = u_{\text{jet}} \\ H_m = H_{\text{jet}} \\ \alpha_i = \alpha_{i_{\text{jet}}} \end{cases} \\ y > a & \begin{cases} u = u_e \\ H_m = H_e \\ \alpha_i = \alpha_{ie} \end{cases} \end{cases} \quad x > 0, \; y \to \infty \quad \begin{cases} u = u_e \\ H_m = H_e \\ \alpha_i = \alpha_{ie} \end{cases} \quad (31)$$

These conditions are supplemented with the symmetry conditions on the jet axis. The solution technique is essentially that employed in the diffusive equilibrium studies.

Under the assumption of equilibrium condensation in the present analysis, the system of equations reduces to the

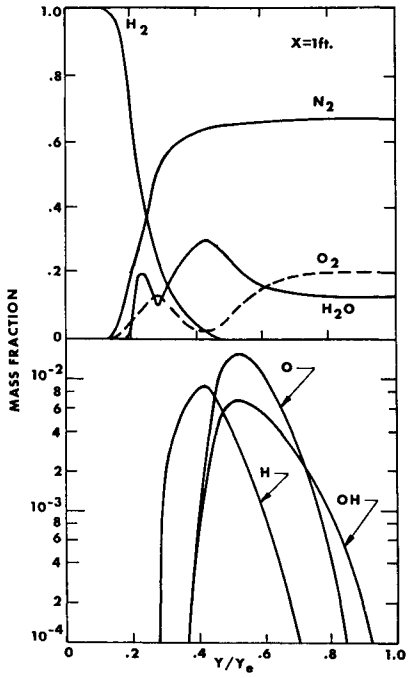

Fig. 5 Distribution of the mass fractions of H_2O, N_2, O, and H_2, (top) and O, H, and OH (bottom).

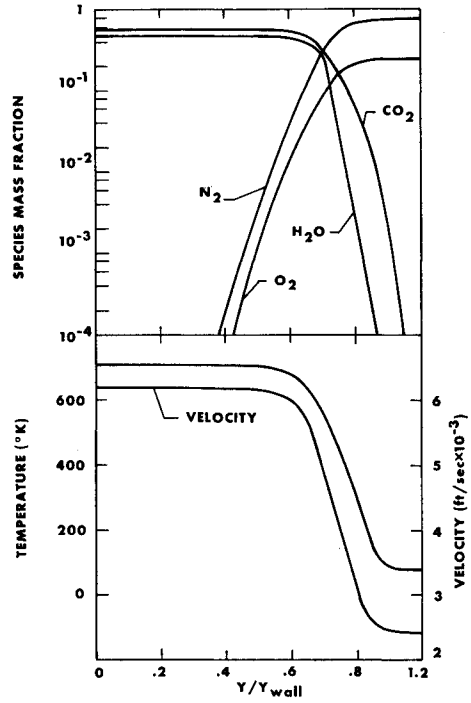

Fig. 7 Velocity and temperature profiles at station A/A jet = 22.

gas phase problem when the temperature is above the saturation value corresponding to the local pressure. For the flow composition here, it is governed by the saturation temperature of H_2O which is well below that required for any of the chemical reactions considered. Should the temperature lie above the saturation value, the calculation is performed using finite rate chemistry.

Results

The frozen diffusion analysis has been applied to the configuration depicted in Fig. 4. The jet is an axisymmetric, fully expanded stream of low-temperature hydrogen and the outer flow is a uniform stream of moist air. The jet temperature is sufficiently low to condense the O_2, N_2, and H_2O after mixing has occurred. The freestream temperatures were chosen above the ignition limit to provide conditions for chemically active two-phase flows. Region A represents the core of pure hydrogen that is virtually unaffected by the diffusion process. In region B mixing has occurred but the temperature levels are well below the required temperature for ignition. This region is predominantly H_2, O_2, and H_2O in two-phase states with only traces of gaseous O, H, and OH. Region C represents a zone of intermediate temperature levels which are above those required for two-phase states and not yet high enough for ignition. Combustion takes place at the higher temperatures which prevail in region D where significant concentrations of all seven species appear. The approach to the freestream state is accompanied by the disappearance of hydrogen and combustion subsides. Therefore, region E is a zone where some mixing has occurred devoid of significant chemical activity.

To study the behavior of a two-phase system with combustion, the freestream temperature and pressure were picked as 1500°K and 110 lb/ft², respectively. The pressure corresponds to an altitude of 20 KM where the hydrogen jet at the temperature of 40°K is in an all gas state. Radial distributions of the pertinent variables are shown in Figs. 5 and 6 which represent the flowfield configuration at a streamwise station where significant chemical and two-phase phenomenon are present. Figure 5 shows the mass fraction distribution of the major components in the flowfield. The appearance of significant chemical reaction is evident by the large increase in the mass fraction of H_2O in the high-temperature region ($900 < T < 1500$°K) Additional evidence of combustion in this region is the depletion of O_2 and H_2 in the vicinity of $y/y_e \cong 0.4$. The corresponding mass fractions of O, H, and OH attain their peak values within this

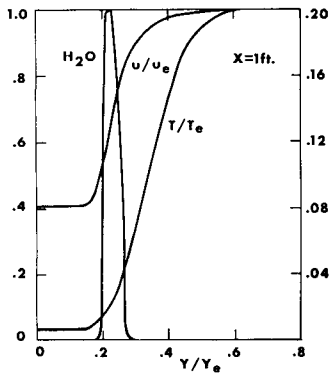

Fig. 6 Distribution of condensed phase mass fraction, velocity, and temperature.

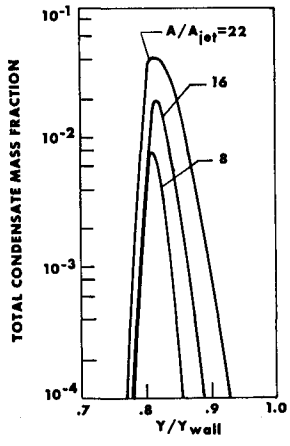

Fig. 8 Condensed water profiles at several downstream stations.

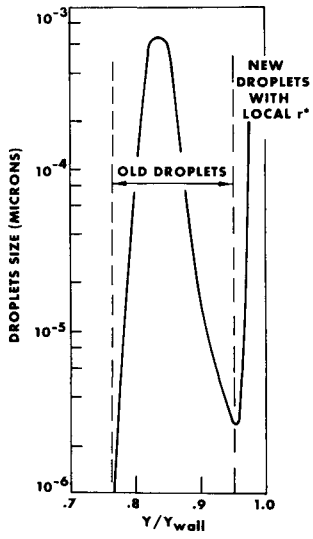

Fig. 9 Condensate size distribution in the first category at $A/A_{jet} = 22$.

combustion zone. The temperature decreases rapidly toward the axis and the flowfield passes through a narrow region where chemical reactions are negligible and condensation has not yet appeared. The H_2O begins condensing nearer the axis and is accompanied by the same behavior of the N_2 and O_2 which has been observed in low-temperature, chemically frozen cases. The H_2O has a second peak concentration here and the N_2 and O_2 show a corresponding depletion due to gas phase diffusion. This peak in the H_2O concentration is associated with the phase separation phenomena, wherein the condensate does not diffuse once it is formed. Figure 6 shows the narrow zone of condensed H_2O and illustrates that to this scale, negligible condensed O_2 and N_2 appear, although trace quantities are present in the flowfield. Also shown in Fig. 6 are the velocity and temperature distributions. Although there is significant chemical activity, the temperature distribution is monotonic showing the capacity of the low-temperature H_2 to absorb the energy released during combustion.

The finite-rate condensation analysis with equilibrium diffusion was used to examine a ducted expansion process with nonuniform initial conditions like that shown in Fig. 1. The primary flow provides a source of hot gaseous H_2O and CO_2 in proportions appropriate to the combustion of a hydrocarbon fuel and oxygen. The surrounding gas is a slight supersonic cold airstream at sea-level pressure and temperature. As the flowfield develops, the gaseous H_2O spreads into the secondary air stream and cools. When saturation conditions are reached, the finite-rate condensation of water vapor begins. Gas phase composition, velocity and static temperature profiles are given in Fig. 7. An indication of the spread of condensate in the radial and streamwise directions is given by Fig. 8. As the flow moves downstream, the amount of condensate and its radial extent increases. The radius distribution of a condensate in the first size category (0 to 10^{-3} μ) is given in Fig. 9. The secondary peak in the vicinity of the wall is due to the creation of "new" droplets as the gaseous H_2O diffuses further into the cold secondary flow.

The condensate between $y/y_w = 0.77$ to 0.95 represents the size variation of "old" droplets created upstream as effected by their growth history. These droplets comprise the majority of condensate present. Near the wall ($y/y_w >$ 0.95) the saturation ratio is relatively high, and the small condensate mass fraction (below 10^{-13}) in this region is essentially comprised of critical sized droplets.

Conclusions

An analysis of two-phase flow has been applied to a variety of problems involving models coupling the chemical, phase transition and mixing processes. Examples are given for hydrogen and hydrocarbon chemical systems in ducted and freejet configurations.

Combustion, phase transition, and phase separation phenomena are shown to be important considerations in analyzing the general two-phase flow problem. These effects are of particular relevance in non-one-dimensional flows including combustion chambers and nozzles involving either nonuniform entrance conditions or employing film cooling.

References

[1] Kliegel, J. R. and Nickerson, G. R., "Flow of Gas-Particle Mixtures in Axially Symmetric Nozzles," *AIAA Progress in Astronautics and Rocketry: Detonation and Two-Phase*, Vol. 6, edited by S. S. Penner and F. A. Williams, Academic Press, New York, 1962, pp. 173–194.

[2] Hoglund, R. F., "Recent Advances in Gas-Particle Flows," *ARS Journal*, No. 32, 1962, pp. 662–671.

[3] Marble, R. E., "Dynamics of a Gas Containing Small Solid Particles," *Combustion and Propulsion, Fifth AGARD Colloquium*, MacMillan, New York, 1963, p. 105.

[4] Carrier, G. F., "Shock Waves in a Dusty Gas," *Journal of Fluid Mechanics*, No. 4, 1955, pp. 376–382.

[5] Edelman, R. and Rosenbaum, H., "Generalized Viscous Multi-Component Multiphase Flow with Application to Laminar and Turbulent Jets of Hydrogen," *AIAA Journal*, Vol. 2, No. 12, 1964, pp. 2104–2110.

[6] Schetz, J. A., "Analysis of the Mixing and Combustion of Gaseous and Particle-Laden Jets in an Airstream," AIAA Paper 69-33, New York, 1969.

[7] Smoot, L. D., Coates, R. L., and Simonsen, J. M., "Mixing and Combustion of Compressible, Particle-Laden Ducted Flows," AIAA Paper 69-460, U.S. Air Force Academy, Colo., 1969.

[8] Edelman, R. B., Schmotolocha, S., and Slutsky, S., "Combustion of Liquid Hydrocarbons in High Speed Airstream," AIAA Paper 70-88, New York, 1970.

[9] Edelman, R., "Turbulent Transport in Polydisperse Systems," TR-735, 1970, General Applied Science Labs. Inc., Westbury, New York.

[10] Edelman, R., Economos, C., and Boccio, J., "An Analytical and Experimental Study of Some Problems in Two-Phase Flows Involving Mixing and Combustion with Application to the B-O-H-N System," AIAA Paper 70-737, San Diego, Calif., 1970.

[11] Wegener, P. and Pouring, A., "Experiments on Condensation of Water Vapor by Homogeneous Nucleation in Nozzles," *The Physics of Fluids*, Vol. 7, No. 3, March 1964.

[12] Edelman, R. B. and Spadaccini, L., "Analytical Investigation of the Effects of Vitiated Air Contamination on Combustion and Hypersonic Airbreathing Engine Ground Tests," AIAA Paper 69-338, Cincinnati, Ohio, 1969.

[13] Freemont, H. A. et al., "Properties of Combustion Gases—Chemical Composition of Equilibrium Mixture (System C_nH_{2n}-Air)," General Electric, Aircraft Gas Turbine Div., Evendale, Ohio, 1955.

[14] Edelman, R., "Diffusion Controlled Combustion for Scramjet Application," AIAA Paper 66-645, Colorado Springs, Colo., 1966.

[15] Moretti, L., "A New Technique for the Numerical Analysis of Non-Equilibrium Flows," *AIAA Journal*, Vol. 3, No. 2, Feb. 1965, pp. 223–229.